## Photon acceleration from Optical to XUV

R. T. Sandberg\* and A. G. R. Thomas<sup>†</sup> Gérard Mourou Center for Ultrafast Optical Sciences, University of Michigan, Ann Arbor, MI 48109, USA (Dated: January 10, 2023)

The propagating density gradients of a plasma wakefield may frequency upshift a trailing witness laser pulse, a process known as 'photon acceleration'. In uniform plasma, the witness laser will eventually dephase because of group delay. We find phase matching conditions for the pulse using a tailored density profile. An analytic solution for a 1d nonlinear plasma wake with an electron beam driver indicates that, even though the plasma density decreases, the frequency shift reaches no asymptotic limit, i.e. is unlimited provided the wake can be sustained. In fully self-consistent 1d particle-in-cell (PIC) simulations, more than 40 times frequency shifts were demonstrated. In quasi-3d PIC simulations frequency shifts up to ten times were observed, limited only by simulation resolution and non-optimized driver evolution. The pulse energy increases in this process, by a factor of five, and the pulse is guided and temporally compressed by group velocity dispersion, resulting in the resulting XUV laser pulse having near-relativistic ( $a_0 \sim 0.4$ ) intensity.

The many applications of bright, coherent extreme ultraviolet (XUV) light have motivated substantial interest in source development, such as the construction of XUV wavelength Free Electron Lasers such as FLASH [1] as well as nonlinear frequency mixing [2], high harmonic generation [3], relativistic flying mirrors [4–6], and XUV lasing [7], to name a few. Another method for generating short wavelength radiation is 'photon acceleration' [8, 9]; the linear, unmagnetized plasma dispersion relation  $\omega^2 = k^2 c^2 + \omega_p^2$ , where  $\omega_p^2 = e^2 n/m_e \varepsilon_0$  for a plasma of number density n, results in the 'quasi-photons' gaining an effective mass  $\hbar\omega_p/c^2$  by analogy with the relativistic energy-momentum relation for particles with mass. In the presence of co-propagating density gradients, the quasi-photons experience local frequency shifts due to spatiotemporal variations in the phase velocity, and are therefore accelerated (i.e. experience an increase in group velocity). The resulting quasi-photon phase space trajectories in plasma wakefields are similar to those of leptons

Photon acceleration can arise as a result of plasma wakefields [8], ionization fronts [11, 12] and even using metamaterials [13], and was measured in ionization front [14] and laser wakefield acceleration experiments [15, 16]. Recent results include cascaded sequences of localized ionizations [17], resulting in large frequency shifts and the use of plasma wakes to downshift radiation to very long wavelengths [18]. Limits to photon acceleration in plasma wakefields in the linear [19] and nonlinear regimes [20] were previously studied, identifying dephasing of the photon beam with respect to the accelerating refractive index gradient placing a ceiling on the frequency shift. Dephasing occurs when the difference between the phase velocity of the wake and the high-frequency photon pulse results in it slipping out of the accelerating refractive index gradient. A recent scheme for overcoming this restriction using an ionization front is dephasingless frequency shift using a 'flying focus,' a combination of a

chirped laser pulse and an achromatic lens for spatiotemporal shaping of a laser pulse [21]. The flying focus was also used to mitigate the analogous process of electron beam dephasing in a plasma wakefield [22], in addition to related spatiotemporally structured focusing schemes [23, 24].

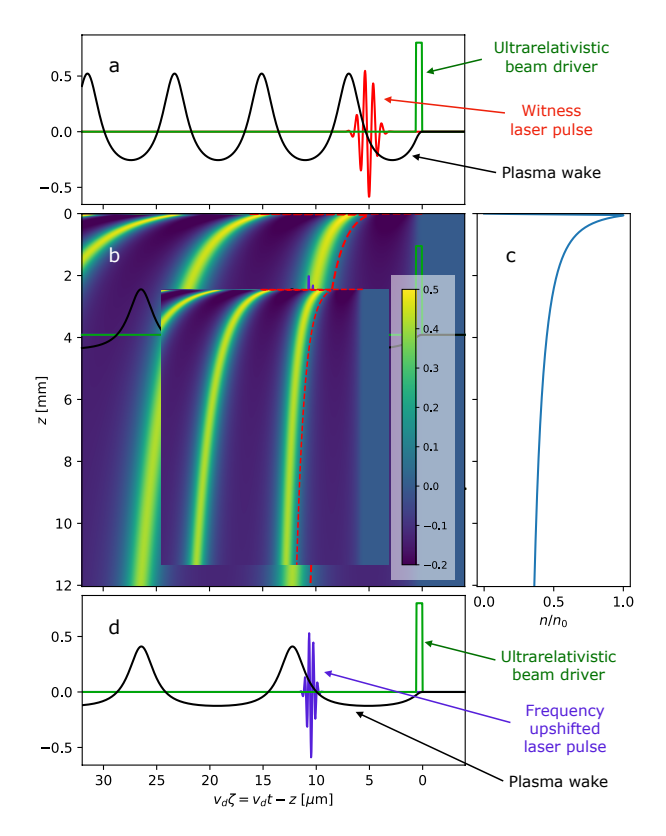


FIG. 1: Schematic for phase matched photon acceleration. (a) / (d) Analytic wakefield behind beam driver at start / end of (c) phase-matching density profile. (b) Analytically calculated plasma wake density (color plot) with density gradient matching witness pulse centroid group delay.

Another method for mitigating dephasing, in the context of electron acceleration is the use of tailored plasma density ramps [25–28]. By having a non-uniform density, the plasma wavelength varies along the propagation length, which allows for locking the accelerating phase with the particle beam. Tailored density ramps were previously suggested as a way of increasing the frequency shifts in photon acceleration [8, 19].

In this Letter, we develop an analytic model for dephasingless photon acceleration in the nonlinear plasma wake regime, based on a tailored plasma density profile. The model shows that if a wake can be sustained for arbitrary distance, there is formally no limit to the frequency shift achievable. The 1d model is verified by comparison with 1d particle-in-cell (PIC) simulations and used to design the density profile for quasi-3d PIC simulations for a broad driver beam, which demonstrates a frequency upshift of an 800 nm witness laser pulse up to 80 nm, Fig. 1. The pulse experiences net energy gain of  $5\times$  to 250 mJ and is compressed, leading to an ultrashort pulse of XUV radiation with near-relativistic intensity, i.e.  $a_0 = eE_0/m_ec\omega_0 \rightarrow 1$ , where  $E_0$  is the peak field of the witness pulse.

A laser pulse that experiences a co-moving plasma density gradient will be upshifted in frequency. From eikonal solutions to the wave equation, well known ray-tracing (photon kinetic) solutions can be used for the temporal variation in the light [9, 29, 30] to relate it to the density gradients generated in a wakefield. We assume that the laser pulse is propagating in a wakefield generated by a relativistic driver (either a relativistic particle beam or second laser pulse) propagating at velocity  $v_d(z)$  and therefore change coordinates from (x, y, z, t) to  $(x, y, z, \zeta = t - \int_0^z dz'/v_d(z'))$  [26]. For a given dispersion relation D, the frequency of an optical mode  $\omega$  propagating in the z direction with wavenumber  $k_z$  will vary with distance propagated z as

$$\frac{d\omega}{dz} = \frac{\partial D/\partial \zeta}{\partial D/\partial k_z} \ . \tag{1}$$

For example, for linear plasma dispersion,  $D=\omega^2-\omega_p^2/\gamma-k^2c^2$ , and assuming that ions are immobile and the variations in the plasma density with respect to  $\zeta$  are much larger than the variations in  $\omega$  and k and can be ignored.

$$\frac{d\omega}{dz} \simeq \frac{1}{2k_z c^2} \frac{\partial(\omega_p^2/\gamma)}{\partial \zeta} \ . \tag{2}$$

Note that the  $\gamma$  factor in the linear dispersion relation is to allow for relativistically streaming electrons rather than, e.g. oscillations in the laser field, and therefore this dispersion relation is considered exact for a weak laser pulse.

For positive frequency shift, the laser pulse must be at a phase in the wake where the density gradient is positive with respect to  $\zeta$ , Fig. 1. However, the laser centroid

moves at the group velocity of the laser pulse and so as the laser pulse shifts in frequency, its group velocity increases and the pulse will change position in the wake. To mitigate dephasing of the photon pulse, we use a tailored density profile (similar to that proposed for mitigating dephasing in electron acceleration [26, 28, 31, 32]) to continuously increase the plasma wavelength and keep the laser pulse experiencing a positive plasma density gradient, Fig. 1.

For convenience, we choose the point where the density perturbation in the wake is zero,  $\delta n=0$ , within the positive gradient region, hereby labelled as  $\zeta_{\delta}$ , as the location of the reference density gradient we are trying to track. This is not the maximum density gradient except in the linear regime, but the maximum is in general slightly behind  $\zeta_{\delta}$ , and using  $\zeta_{\delta}$  simplifies the analysis. It can be shown that the maximum refractive index gradient occurs where the electric field of the wake is zero, which is close to where the density perturbation goes to zero. It can also be shown that the refractive index gradient is equal to the density gradient at the point where  $\delta n=0$  for a 1d wake.

To keep the pulse experiencing the greatest possible frequency shift, we require  $\zeta_{\text{centroid}} = \zeta_{\delta}$  for all times, where  $\zeta_{\text{centroid}}$  denotes the center of the witness laser pulse or, expressed in differential form,

$$\frac{d\zeta_{\text{centroid}}}{dz} = \frac{d\zeta_{\delta}}{dz} \Rightarrow \frac{1}{v_{\text{centroid}}} - \frac{1}{v_d} = \frac{d\zeta_{\delta}}{dn} \frac{dn}{dz} .$$
 (3)

The quantity n refers to the unperturbed plasma density ahead of the driver and is a function of z. For an ultrarelativistic particle beam driver, we make the approximation  $v_d \to c$ . Assuming that the laser pulse moves at the linear group velocity and the plasma is underdense,  $\omega_p^2/\omega^2 \ll 1$ , we obtain an equation relating the z profile of the plasma number density to the variation in the wake position of the zero density perturbation  $\zeta_\delta$  with plasma density,

$$\frac{dn}{dz} \simeq \frac{1}{2c} \frac{\omega_p^2}{\omega^2} \left[ \frac{d\zeta_\delta}{dn} \right]^{-1} . \tag{4}$$

Note that  $\gamma(\zeta_{\delta}) = 1$ , where the density perturbation is zero.

Here, we derive the phase-matching condition for a one-dimensional (1d) nonlinear plasma wake, which we find is also accurate to describe the three-dimensional case for a broad driver  $(k_p\sigma_r\gg 1)$ , where  $k_p=\omega_p/c$  and  $\sigma_r$  is the is the root-mean-square beam radius. Under the assumption that  $d\log(n)/dz\ll k_p(z)$  for all z, i.e. the plasma density gradients are long compared to the wake period scale, to lowest order the wake may be assumed to follow the uniform plasma solution with local density n(z). Hence, we write the perturbed density of the wake  $n_w(\zeta;z)$  as a function of  $\zeta$  parameterized by z, i.e. by the local density n(z).

$$\tan \varphi_{st} = \frac{-E_d}{p_d} \sqrt{\frac{\gamma_d - 1}{2}} \,, \tag{5}$$

where  $E_d$ ,  $p_d$ , and  $\gamma_d$  are the electric field, momentum, and Lorentz factor of the plasma at the end of the drive beam. These quantities are obtained from solutions to the fluid equations with the drive beam density included [34]. The position  $\zeta_{\delta}$ , measured from the *leading* edge of the drive beam, may be expressed as

$$\zeta_{\delta} = \zeta(3\pi/2) - \zeta(\varphi_{st}) + \tau_d , \qquad (6)$$

where  $\zeta(\varphi)$  is the position in the undriven wake as a function of a periodic parametric coordinate  $\varphi$ , with  $\varphi(0)$  corresponding to a density maximum. The function  $\zeta(\varphi)$  is defined implicitly by  $\zeta(\varphi) = (2/\kappa')E(\varphi,\kappa) - \kappa' F(\varphi,\kappa) - (2\kappa/\kappa')\sin\varphi$ , where  $F(\varphi,\kappa)$  and  $E(\varphi,\kappa)$  are elliptic integrals of the first and second kind,  $\kappa^2 = (\gamma_m - 1)/(\gamma_m + 1)$  and  $\kappa'^2 = 1 - \kappa^2$ . Hence, the change in the location of the phase-matched refractive index gradient used in Eqn. 4,  $d\zeta_\delta/dn$ , is defined implicitly using Eqns. 5 and 6. The plasma wake density gradient at  $\zeta_\delta$  is given by

$$\left. \frac{\partial n_w}{\partial \zeta} \right|_{\zeta = \zeta_\delta} = n\sqrt{2\left[\gamma_m - 1\right]} \ . \tag{7}$$

In normalized units, combining Eqns. 2 and 7 yields

$$\frac{d\omega^2}{dz} \simeq n^{3/2} \sqrt{2 \left[ \gamma_m - 1 \right]} \,, \tag{8}$$

and Eqn. 4 is

$$\frac{dn}{dz} \simeq \frac{1}{2} \frac{n}{\omega^2} \left[ \frac{d\zeta_\delta}{dn} \right]^{-1} . \tag{9}$$

Eqns. (8) and (9) are a coupled system of differential equations that can be evaluated to determine the density profile and expected frequency shift for phase matched photon acceleration driven by an ultrarelativistic beam driver of arbitrary length and density. Finding the variation of  $\zeta_{\delta}$  with density in the nonlinear case is a challenge as it is the solution of an implicit equation. Insight can

be gained, however, by using an ultrashort driver approximation, for which an analytic solution can be found.

The ultrashort driver approximation means fixing  $A = n_d \tau_d$  and letting  $\tau_d \to 0$ , so that  $n_d = A/\tau_d \to \infty$ . In this limit, the maximum amplitude of the wave reduces to  $\gamma_m(n;A) = 1 + A^2/2n$  and the phase is  $\varphi_{st} = \pi/2$ .

Eqns. (8) and (9) may be combined and directly integrated to obtain

$$\omega(n) = \omega_0 \exp\left[A\left(\zeta_\delta(n) - \zeta_{\delta 0}\right)\right] \tag{10}$$

defined for n in  $(0, n_0]$  where  $n(0) = n_0$ . Since  $d\omega^2/dz > 0$  and dn/dz < 0, there are no fixed points or periodic orbits and so, by the Poincaré-Bendixon theorem [35], there are no limit sets to the orbits. Furthermore, as  $n \to 0$ ,  $\zeta_{\delta}(n) \to \infty$  and so we see from Eqn. 10 that  $\omega(n) \to \infty$ . We can determine the evolution of the system in terms of propagation distance z via the implicitly defined equation for n(z),

$$z = 2\omega_0^2 \int_{n_0}^n \frac{1}{n'} \frac{d\zeta_\delta}{dn'} e^{2A(\zeta_\delta(n) - \zeta_{\delta 0})} dn' . \tag{11}$$

For a moderate strength driver, A < 1, the location of the zero density perturbation,  $\zeta_{\delta}$ , can be described accurately by the expansion

$$\zeta_{\delta} = \frac{\pi}{n^{1/2}} + \frac{2A}{n} + \frac{3\pi}{16} \frac{A^2}{n^{3/2}} + \cdots$$
(12)

To verify the model, we ran a number of 1d PIC simulations using the OSIRIS 4.0 framework [36]. Using normalized units, these were performed for a one-component electron plasma in a box of width  $L_z=35.0$  with  $N_z=120,096$  meshpoints, a timestep  $\Delta t=0.000254$ , and 4 particles-per-cell, with the density profile having a short linear ramp to  $n=n_0$  followed by a tailored density profile n(z) following the solution to Eqn. 11, i.e. similar to Fig. 1c. The beam driver had a square profile, the witness laser pulse a gaussian profile with strength  $a_0=0.1$ , duration  $\tau_L=1$  and initial central frequency  $\omega_0/\omega_p=5$ , i.e. a normalizing plasma density  $n_0=7\times 10^{19}$  cm<sup>-3</sup> for a 800 nm laser wavelength.

Fig. 2a shows the results from Simulation A, the witness laser spectrum as a function of z for a driver with duration  $\tau_d=1,\ n_d=0.8$  and a beam energy  $\gamma_d mc^2=50$  GeV. The entire witness laser spectrum is shifted to  $\omega/\omega_0>40$ . The red curve shows the analytic solution given by Eqn. 10, the black curves show the mean and peak frequency. Until 85 mm propagation, these track the analytic solution very precisely. After 85 mm, the drive beam electrons are decelerated at the rear, leading to erosion of the trailing edge, which disrupts the wake. For longer propagation numerical dispersion becomes an issue at the high frequencies of the pulse.

To address the applicability of the model to realistic 3d conditions, we used the numerical-dispersion free

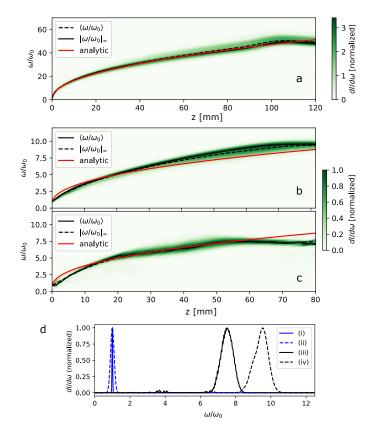


FIG. 2: Witness laser pulse spectrum as a function of propagation z for (a) 1d PIC and (b)/(c) Quasi-3d PIC simulations described in the text. Lines in red are the theoretical curves given by Eqns (10-12). Black and black-dashed lines show the mean and peak frequencies as a function of z. (d) Shows initial (i, ii) and maximum shift (iii, iv) spectra for quasi-3d simulations with (i/iii) 20 GeV beam and (ii/iv) 50 GeV beam driver.

quasi-3d PIC code FBPIC [37]. To make the connection to real parameters, we express values in MKS units for the quasi-3d simulations. In Simulation B shown in Fig. 2b, the drive electron beam has a square profile longitudinally and gaussian profile transversely with duration  $\tau_d = 2$  fs, focused radial extent  $\sigma_r = 32 \ \mu \text{m}$ , divergence  $\sigma_{r'} = 0.4 \text{ mrad}$ , peak density  $n_{d0} = 1.39 \times 10^{19} \text{ cm}^{-3}$ , i.e. such that A = 0.38, and peak beam energy  $\gamma_d mc^2 =$ 50 GeV with relative spread  $\sigma_z/\gamma_d = 0.1\%$ . The linearly polarized witness laser has a normalized field strength parameter  $a_0 = 1$  and initial wavelength  $\lambda_{L0} = 800$  nm, corresponding to a peak intensity  $I = 2.1 \times 10^{18} \text{ Wcm}^{-2}$ , a pulse width  $\tau_L = 4$  fs (similar few cycle laser pulses at this intensity have been demonstrated experimentally [31]), and a spot size of  $w_0 = 2\lambda_{p0} = 20\lambda_{L0} = 16 \ \mu\text{m}$ , starting with its centroid  $\zeta_{\rm cent} = 6.6 \ \mu \rm m/c$  behind the front of the electron drive beam. For these parameters,  $\zeta_{\delta} = 5.4 \ \mu \text{m/c}$ . We use the plasma density profile shown in Fig. 1 and determined by equations (10) and (11),

scaled by  $n_0 = 1.74 \times 10^{19} \text{ cm}^{-3}$ , i.e.  $\omega_0/\omega_p = 10$ .

Simulations were run using  $3200 \times 120$  meshpoints and 2 angular modes. This gives 85 cells per  $\lambda_{L0}$ , which therefore requires a dispersion-free-solver or numerical dispersion would be an impediment. For the electrons we use  $2 \times 2$  particles per cell (ppc) in the z and r directions and 8 ppc in the azimuthal direction. The results of the quasi-3d simulation can be seen in Fig. 2. (b) shows the spectrum as a function of length propagated in the simulation. The spectrum is normalized to its peak at each z. Overlaid is the theoretical model of Eqns (10-12) (red line), which predicts the shift of the photons well, except for discrepancies arising from beam focusing, resulting in small modification to the wake wavelength. (d) shows the initial (ii) and final (iv) spectrum. As well as showing that the pulse maintains a narrow bandwidth, the amplitude of the spectrum has increased, i.e., the energy of the laser pulse increased. The drive beam loses 25 J of energy over the course of the simulation while the laser pulse, initially having 50 mJ, gains 200 mJ for about 1% energy transfer efficiency, which could be increased by optimization of the driver. Note that overall pulse energy gain is not unexpected, as to within the quasistatic approximation, local field action is conserved [39], and so the energy gain by the pulse would be expected to scale with the frequency increase. In the 1d simulation, the energy gain is proportional to the frequency increase. In the quasi-3d simulations, the nearly  $10\times$  frequency shift results in a lower  $5 \times$  pulse energy gain, because of losses due to diffraction/dispersion.

Owing to the nonlinear wake, the back of the pulse sees a steeper plasma gradient than the front of the pulse. The pulse develops significant up-chirp, which, together with dispersion, leads to a 2.7× compression of the pulse from an initial duration of  $\tau_L=4$  fs to 1.7 fs. The intensity sees a significant increase of  $20\times$  from an initial intensity  $I=2\times 10^{18}~{\rm W/cm^2}$  to  $4\times 10^{19}~{\rm W/cm^2}$ , a near-relativistic intensity corresponding to  $a_0=0.4$  at 80 nm, in part because the wake has an approximately parabolic transverse profile and acts as an effective guiding channel. The simulation is shown ending at 80 mm. Beyond this length, the beam driver has lost sufficient energy to break up and the simulation is near the resolution limit for the maximum frequency.

Lastly, to model a potential near-term experiment, we ran Simulation C for a 20 GeV beam, which is closer to the parameters of the current SLAC FACET-II facility [38], and a longer,  $\tau_L=25$  fs, witness laser pulse. The beam divergence was adjusted to  $\sigma_{r'}=0.75$  mrad and  $a_0=0.1$ . In addition, to compensate for increased defocusing of the beam, which results in detuning of the wake wavelength, we adjusted the electron beam focus to be 20 mm into the simulation. As shown in Fig. 2c, the laser spectrum still follows the analytic solution to around 55 mm, where the beam defocusing starts to be significant and the pulse both dephases and diffracts. (d) shows the

Sim.	$\gamma_d m_e c^2 \text{ [GeV]}$	A	$\sigma'_r$ [mrad]	$a_0$	$\tau_L$ [fs]	$n_0 \ [{\rm cm}^{-3}]$
A	50	0.8	N/A	0.1	2 fs	$7 \times 10^{19}$
В	50	0.38	0.4	1	4  fs	$1.74 \times 10^{19}$
С	20	0.38	0.75	0.1	25  fs	$1.74 \times 10^{19}$

TABLE I: Parameters for the three simulations described in text. All are chosen to have comparable driver length  $\tau_d = 2$  fs. For simulation 1 normalized units are converted using  $\lambda = 800$  nm.

initial spectrum (i) and spectrum at 55 mm (ii), showing the spectrum is still shifted by nearly  $8\times$ . The steep gradient rapidly introduces a strong chirp that leads to compression of the majority of the pulse to few cycles in the initial stages. These three simulations are summarized in Table I.

In summary, we have demonstrated a scheme for large frequency upshift of a laser pulse using the wake generated by a relativistic particle beam propagating through a tailored plasma density profile. Our analytic model predicts arbitrary frequency shift limited only by depletion of the drive beam. Quasi-3d simulation results directly demonstrated a  $10\times$  frequency shift with 1% energy transfer efficiency. The wake itself serves as a wave guide. Combined with relativistic self-focusing and the lengthening of the Rayleigh range as the frequency increases, the pulse is guided for the duration of the interaction.

For a simple unoptimized focused single-beam driver, as used in the demonstrations here, it will lose energy at near constant rate in the wake. By equating the length over which depletion occurs for a single driver with the frequency gain of the witness, the maximum frequency shift is  $\Delta\omega \simeq R\omega_p\sqrt{\gamma_d}$ , where R is a number of order unity representing the ratio of the magnitude of the gradient in n at the witness position to the maximum electric field in the driver, similar to the transformer ratio in PWFA [40]. Another limit is the effective Rayleigh length of the focused electron beam. These are not fundamental limits as there is much scope for overcoming depletion and defocusing, including advancements in spatiotemporally evolving electron beam drivers [41], stabilization with magnetic fields [42], or transversely matched beams [43], for example. For the study here, we were not able to explore higher frequency shifts due to numerical limits in resolution/simulation size. To push to even higher frequency shifts will require the development of new and more sophisticated numerical tools.

This work was supported by AFOSR grant FA9550-19-1-0072 and NSF grant 1804463. Computational resources were provided by Advanced Research Computing at the University of Michigan.

- \* rsandberg@lbl.gov, presently at Lawrence Berkeley National Laboratory
- † agrt@umich.edu
- [1] Jörg Rossbach, Jochen R. Schneider, and Wilfried Wurth. 10 years of pioneering x-ray science at the free-electron laser flash at desy. *Physics Reports*, 808:1-74, 2019. ISSN 0370-1573. doi: https://doi.org/10.1016/j.physrep.2019.02.002. URL https://www.sciencedirect.com/science/article/pii/S0370157319300663. 10 years of pioneering X-ray science at the Free-Electron Laser FLASH at DESY.
- [2] M A Khokhlova and V V Strelkov. Highly efficient XUV generation via high-order frequency mixing. New Journal of Physics, 22(9):093030, sep 2020. doi: 10.1088/1367-2630/abae89. URL https://doi.org/10. 1088/1367-2630/abae89.
- [3] Zenghu Chang, Andy Rundquist, Haiwen Wang, Margaret M. Murnane, and Henry C. Kapteyn. Generation of coherent soft x rays at 2.7 nm using high harmonics. *Phys. Rev. Lett.*, 79:2967–2970, Oct 1997. doi: 10.1103/PhysRevLett.79.2967. URL https://link.aps.org/doi/10.1103/PhysRevLett.79.2967.
- [4] Sergei V. Bulanov, Timur Esirkepov, Toshiki Tajima. Light Intensification towards the Schwinger Limit. Phys. Rev. Lett., 91:085001-085004, Aug 2003. doi: 10.1103/PhysRevLett.91.085001. URL https://link.aps.org/doi/10.1103/PhysRevLett.91.085001.
- [5] M. Kando, A. S. Pirozhkov, K. Kawase, T. Zh. Esirkepov, Y. Fukuda, H. Kiriyama, H. Okada, I. Daito, T. Kameshima, Y. Hayashi, H. Kotaki, M. Mori, J. K. Koga, H. Daido, A. Ya. Faenov, T. Pikuz, J. Ma, L. M. Chen, E. N. Ragozin, T. Kawachi, Y. Kato, T. Tajima, and S. V. Bulanov. Enhancement of Photon Number Reflected by the Relativistic Flying Mirror. Phys. Rev. Lett., 103:235003-235007, Dec 2009. doi: 10.1103/PhysRevLett.103.235003. URL https://link.aps.org/doi/10.1103/PhysRevLett.103.235003.
- [6] S. V. Bulanov, T. Zh. Esirkepov, and M. Kando. Relativistic mirrors in plasmas. Novel results and perspectives *Physics-Uspekhi*, 56:429, May 2013. doi: 10.3367/UFNe.0183.201305a.0449. URL https://dx.doi.org/10.3367/UFNe.0183.201305a.0449.
- [7] B. R. Benware, C. D. Macchietto, C. H. Moreno, and J. J. Rocca. Demonstration of a high average power table-top soft x-ray laser. *Phys. Rev. Lett.*, 81:5804–5807, Dec 1998. doi:10.1103/PhysRevLett.81.5804. URL https://link.aps.org/doi/10.1103/PhysRevLett.81.5804.
- [8] S. C. Wilks, J. M. Dawson, W. B. Mori, T. Katsouleas, and M. E. Jones. Photon accelerator. *Physical Review Letters*, 62(22), 2600-2603, 1989. ISSN 0031-9007.
- [9] Jose Tito Mendonca. Theory of photon acceleration. Institute of Physics Pub, 2001. ISBN 0750307110.
- [10] T. Esirkepov, S. V. Bulanov, M. Yamagiwa, and T. Tajima. Electron, positron, and photon wakefield acceleration: Trapping, wake overtaking, and ponderomotive acceleration. *Physical Review Letters*, 96(1):014803, 1 2006. ISSN 10797114. doi: 10.1103/PhysRevLett.96.014803.
- [11] E. Esarey, G. Joyce, and P. Sprangle. Frequency upshifting of laser pulses by copropagating ionization fronts. *Physical Review A*, 44(6):3908–3911, 9 1991. ISSN

- $10502947.\ doi: 10.1103/PhysRev A.44.3908.$
- [12] Luis Oliveira e Silva and Jose Tito Mendonca. Photon acceleration in superluminous and accelerated ionization fronts. *IEEE Transactions on Plasma Science*, 24(2):316– 322, 4 1996. ISSN 00933813. doi:10.1109/27.509995.
- [13] Maxim R. Shcherbakov, Kevin Werner, Zhiyuan Fan, Noah Talisa, Enam Chowdhury, and Gennady Shvets. Photon acceleration and tunable broadband harmonics generation in nonlinear time-dependent metasurfaces. Nature Communications, 10(1):1345, 2019. doi: 10.1038/s41467-019-09313-8. URL https://doi.org/ 10.1038/s41467-019-09313-8.
- [14] J. M. Dias, C. Stenz, N. Lopes, X. Badiche, F. Blasco, A. Dos Santos, L. Oliveira e Silva, A. Mysyrowicz, A. Antonetti, and J. T. Mendonça. Experimental evidence of photon acceleration of ultrashort laser pulses in relativistic ionization fronts. *Phys. Rev. Lett.*, 78:4773–4776, Jun 1997. doi:10.1103/PhysRevLett.78.4773. URL https: //link.aps.org/doi/10.1103/PhysRevLett.78.4773.
- [15] C. W. Siders, S. P. Le Blanc, D. Fisher, T. Tajima, M. C. Downer, A. Babine, A. Stepanov, and A. Sergeev. Laser wakefield excitation and measurement by femtosecond longitudinal interferometry. *Phys. Rev. Lett.*, 76:3570–3573, May 1996. doi: 10.1103/PhysRevLett.76.3570. URL https://link.aps. org/doi/10.1103/PhysRevLett.76.3570.
- [16] C. D. Murphy, R. Trines, J. Vieira, A. J. W. Reitsma, R. Bingham, J. L. Collier, E. J. Divall, P. S. Foster, C. J. Hooker, A. J. Langley, P. A. Norreys, R. A. Fonseca, F. Fiuza, L. O. Silva, J. T. Mendonca, W. B. Mori, J. G. Gallacher, R. Viskup, D. A. Jaroszynski, S. P. D. Mangles, A. G. R. Thomas, K. Krushelnick, and Z. Najmudin. Evidence of photon acceleration by laser wake fields. *Physics of Plasmas*, 13(3):033108, 2006. doi: 10.1063/1.2178650. URL https://doi.org/10.1063/1.2178650.
- [17] Matthew R. Edwards, Kenan Qu, Qing Jia, Julia M. Mikhailova, and Nathaniel J. Fisch. Cascaded chirped photon acceleration for efficient frequency conversion. *Physics of Plasmas*, 25(5), 5 2018. ISSN 1070-664X.
- [18] Zan Nie, Chih Hao Pai, Jianfei Hua, Chaojie Zhang, Yipeng Wu, Yang Wan, Fei Li, Jie Zhang, Zhi Cheng, Qianqian Su, Shuang Liu, Yue Ma, Xiaonan Ning, Yunxiao He, Wei Lu, Hsu Hsin Chu, Jyhpyng Wang, Warren B. Mori, and Chan Joshi. Relativistic single-cycle tunable infrared pulses generated from a tailored plasma density structure. *Nature Photonics*, 12(8):489–494, 8 2018. ISSN 17494893. doi:10.1038/s41566-018-0190-8.
- [19] E. Esarey, A. Ting, and P. Sprangle. Frequency shifts induced in laser pulses by plasma waves. *Physical Re*view A, 42(6):3526-3531, 9 1990. ISSN 10502947. doi: 10.1103/PhysRevA.42.3526. URL https://journals. aps.org/pra/abstract/10.1103/PhysRevA.42.3526.
- [20] V. A. Mironov, A. M. Sergeev, E. V. Vanin, G. Brodin, and J. Lundberg. Upper limits for frequency upconversion in the nonlinear photon accelerator. *Physical Review A*, 46(10):R6178-R6180, 11 1992. ISSN 1050-2947. doi:10.1103/PhysRevA.46.R6178. URL https://link.aps.org/doi/10.1103/PhysRevA.46.R6178.
- [21] A. J. Howard, D. Turnbull, A. S. Davies, P. Franke, D. H. Froula, and J. P. Palastro. Photon Acceleration in a Flying Focus. *Physical Review Letters*, 123(12):124801, 9 2019. ISSN 10797114. doi: 10.1103/PhysRevLett.123.124801.

- [22] J. P. Palastro, J. L. Shaw, P. Franke, D. Ramsey, T. T. Simpson, and D. H. Froula. Dephasingless laser wakefield acceleration. *Phys. Rev. Lett.*, 124:134802, Mar 2020. doi: 10.1103/PhysRevLett.124.134802. URL https://link.aps.org/doi/10.1103/PhysRevLett.124.134802.
- [23] Alexander Debus, Richard Pausch, Axel Huebl, Klaus Steiniger, René Widera, Thomas E. Cowan, Ulrich Schramm, and Michael Bussmann. Circumventing the Dephasing and Depletion Limits of Laser-Wakefield Acceleration. *Physical Review X*, 99: 031044, 2019. ISSN 21603308.
- [24] C. Caizergues, Smartsev, V. Malka, and C. Thaury. Phase-locked laser-wakefield elec-14(8):475tron acceleration. Nature Photonics, 2020. doi:10.1038/s41566-020-0657-2. URL https://doi.org/10.1038/s41566-020-0657-2.
- [25] S. V. Bulanov, V. A. Vshivkov, G. I. Dudnikova, N. M. Naumova, F. Pegoraro, and I. V. Pogorelsky. Laser acceleration of charged particles in inhomogeneous plasmas i. *Plasma Physics Reports*, 23(4):259-269, 1997. doi:DOI:101134/1952453. URL http://inis.iaea.org/search/search.aspx?orig\_q=RN:35015260.
- [26] P. Sprangle, B. Hafizi, J. R. Peñano, R. F. Hubbard, A. Ting, C. I. Moore, D. F. Gordon, A. Zigler, D. Kaganovich, and T. M. Antonsen. Wakefield generation and GeV acceleration in tapered plasma channels. *Physical Review E*, 63(5):056405, 4 2001. ISSN 1063-651X. doi:10.1103/PhysRevE.63.056405.
- [27] E. Guillaume, A. Döpp, C. Thaury, K. Ta Phuoc, A. Lifschitz, G. Grittani, J.-P. Goddet, A. Tafzi, S. W. Chou, L. Veisz, and V. Malka. Electron Rephasing in a Laser-Wakefield Accelerator. *Physical Review Letters*, 115(15):155002, 10 2015. ISSN 0031-9007. doi: 10.1103/PhysRevLett.115.155002.
- [28] S. V. Bulanov, T. Zh. Esirkepov, Y. Hayashi, H. Kiriyama, J. K. Koga, H. Kotaki, M. Mori, and M. Kando. On some theoretical problems of laser wake-field accelerators. *Journal of Plasma Physics*, 82(3):905820308, 6 2016. ISSN 0022-3778. doi: 10.1017/S0022377816000623.
- [29] Steven Weinberg. Eikonal Method in Magnetohydrodynamics. *Physical Review*, 126(6):1899–1909, 6 1962. ISSN 0031-899X. doi:10.1103/PhysRev.126.1899.
- [30] Jose Tito Mendonca. Vlasov equation for photons and quasi-particles in a plasma. The European Physical Journal D, 68(4), 4 2014. ISSN 1434-6060.
- [31] D. Guénot, D. Gustas, A. Vernier, B. Beaurepaire, F. Böhle, M. Bocoum, M. Lozano, A. Jullien, R. Lopez-Martens, A. Lifschitz, and J. Faure. Relativistic electron beams driven by kHz single-cycle light pulses. *Nature Photonics*, 11(5):293–296, 5 2017. ISSN 1749-4885. doi: 10.1038/nphoton.2017.46.
- [32] J. Kim, V. L. J. Phung, K. Roh, M. Kim, K. Kang, and H. Suk. Development of a density-tapered capillary gas cell for laser wakefield acceleration. *Review of Scientific Instruments*, 92(2):023511, 2 2021. ISSN 0034-6748. doi: 10.1063/5.0009632.
- [33] A.I. Akhiezer and R.V. Polovin. Theory of wave motion of an electron plasma. *Journal of Experimental and Theoretical Physics*, 3(5):696–705, 1956.
- [34] J. B. Rosenzweig. Nonlinear plasma dynamics in the plasma wake-field accelerator. *Physical Review Let*ters, 58(6):555-558, 2 1987. ISSN 0031-9007. doi: 10.1103/PhysRevLett.58.555. URL https://link.aps.

- org/doi/10.1103/PhysRevLett.58.555.
- [35] R. A. Struble. Nonlinear Differential Equations. Dover Books on Mathematics. Dover Publications, 2018. ISBN 9780486817545.
- [36] R. A. Fonseca, et al, in Computational Science-ICCS 2002, Lecture Notes in Computer Science, Vol. 2331: 342–351 (2002).
- [37] Rémi Lehe, Manuel Kirchen, Igor A. Andriyash, Brendan B. Godfrey, and Jean Luc Vay. A spectral, quasicylindrical and dispersion-free Particle-In-Cell algorithm. Computer Physics Communications, 203:66–82, 6 2016. ISSN 00104655. doi:10.1016/j.cpc.2016.02.007.
- [38] V. Yakimenko, L. Alsberg, E. Bong, G. Bouchard, C. Clarke, C. Emma, S. Green, C. Hast, M. J. Hogan, J. Seabury, N. Lipkowitz, B. O'Shea, D. Storey, G. White, and G. Yocky. FACET-II facility for advanced accelerator experimental tests. *Physical Review Accelera*tors and Beams, 22(10):101301, 10 2019. ISSN 2469-9888. doi:10.1103/PhysRevAccelBeams.22.101301.
- [39] W.B. Mori. The physics of the nonlinear optics of plasmas at relativistic intensities for short-pulse lasers. IEEE

- $\label{eq:Journal of Quantum Electronics} Journal of Quantum Electronics, 33(11):1942–1953, 1997. \\ ISSN 00189197. \\ \ doi:10.1109/3.641309.$
- [40] Chen, Pisin and Su, J. J. and Dawson, J. M. and Bane, K. L. F. and Wilson, P. B. Energy Transfer in the Plasma Wake-Field Accelerator. *Phys. Rev. Lett.*, 56(12):1252– 1255, 1986.
- [41] Fei Li, Thamine N. Dalichaouch, Jacob R. Pierce, Xinlu Xu, Frank S. Tsung, Wei Lu, Chan Joshi, and Warren B. Mori. Ultra-bright electron bunch injection in a plasma wakefield driven by a superluminal flying focus electron beam. *Phys. Rev. Lett.*, 128(17):174803, 2022.
- [42] Su, J. J. and Katsouleas, T. and Dawson, J. M. and Chen, P. and Jones, M. and Keinigs, R. Stability of the Driving Bunch in the Plasma Wakefield Accelerator. *IEEE Transactions on Plasma Science*, 15(2):192-198, 1987.
- [43] M A Baistrukov and K V Lotov. Evolution of equilibrium particle beams in plasma under external wakefields. Plasma Physics and Controlled Fusion, 64(7): 075003, 2022.